

SESSION 4
CURVED ELEMENTS

Session Chairman

J. F. Besseling

**Technological University
Delft, Holland**

Contrails

**CURVED THICK SHELL AND MEMBRANE ELEMENTS WITH PARTICULAR REFERENCE
TO AXISYMMETRIC PROBLEMS**

Sohrabuddin Ahmad*

Bruce M. Irons**

Olgierd C. Zienkiewicz***

Civil Engineering Division,
University of Wales,
Swansea, Gt. Britain.

General curved isoparametric elements in two and three dimensions are degenerated to deal with axi-symmetric and arbitrary shells. By introducing only some of the usual Navier assumptions, these new shell elements can include shear as well as bending deformations. It is shown that, even for very thick shells, excellent accuracy is retained. By further degeneration membrane situations are dealt with.

* Research Student

** Lecturer

*** Professor (Head of Department)

SECTION I

INTRODUCTION

In several previous publications by the Numerical Analysis Group at Swansea (References 1, 2, 3, 4, and 5) the methodology of generating curved, 'isoparametric' elements was fully explained. By suitable transformations, curvilinear coordinates within such elements are generated and, using numerical integration, the element properties can be determined. Two-dimensional problems of plane stress or strain, axisymmetric problems (Reference 3), and fully three-dimensional problems (References 4 and 5) can be treated, using elements of the families shown in Figure 1 and 2.

Evidently curved shells can be attempted simply by making such two- or three-dimensional elements thin. Indeed up to a point this has proved successful in practice; for instance, an axisymmetric solid program based on the elements of Figure 1, b and c has been used with a length-thickness ratio of 50 or more. Two limitations arose however. In the first place round-off errors occur with very large length-thickness ratios. In the second place, an unnecessarily large number of degrees of freedom are carried, because simplifying constraints are usually introduced in shell analyses. For instance, even in an axisymmetric problem using elements of Type 1c, there are 8 degrees of freedom within the shell thickness, whereas with thin shell assumptions only three would strictly be necessary. Further, for membrane situations the number of degrees of freedom may be reduced even more.

This paper deals with degenerate versions of these general elements for shell problems. In the early sections axisymmetric shell situations are treated and later the process is extended to cover general shells.

In the 'degeneration' process, two assumptions are made. Firstly, the original normals to the middle surface are taken as inextensible and straight. Secondly, the elastic modulus in the normal direction is taken as zero, to avoid normal stresses.

The above assumptions are compatible with thin shell theory, but they allow the normals to rotate relative to the middle surface after deformation. Thus a measure of shear deformation of the shell is retained. Introducing a slight 'correction factor' to the shear deformation, it appears that the answers are consistent with Reissner's (Reference 6) theory of plate in practical applications.

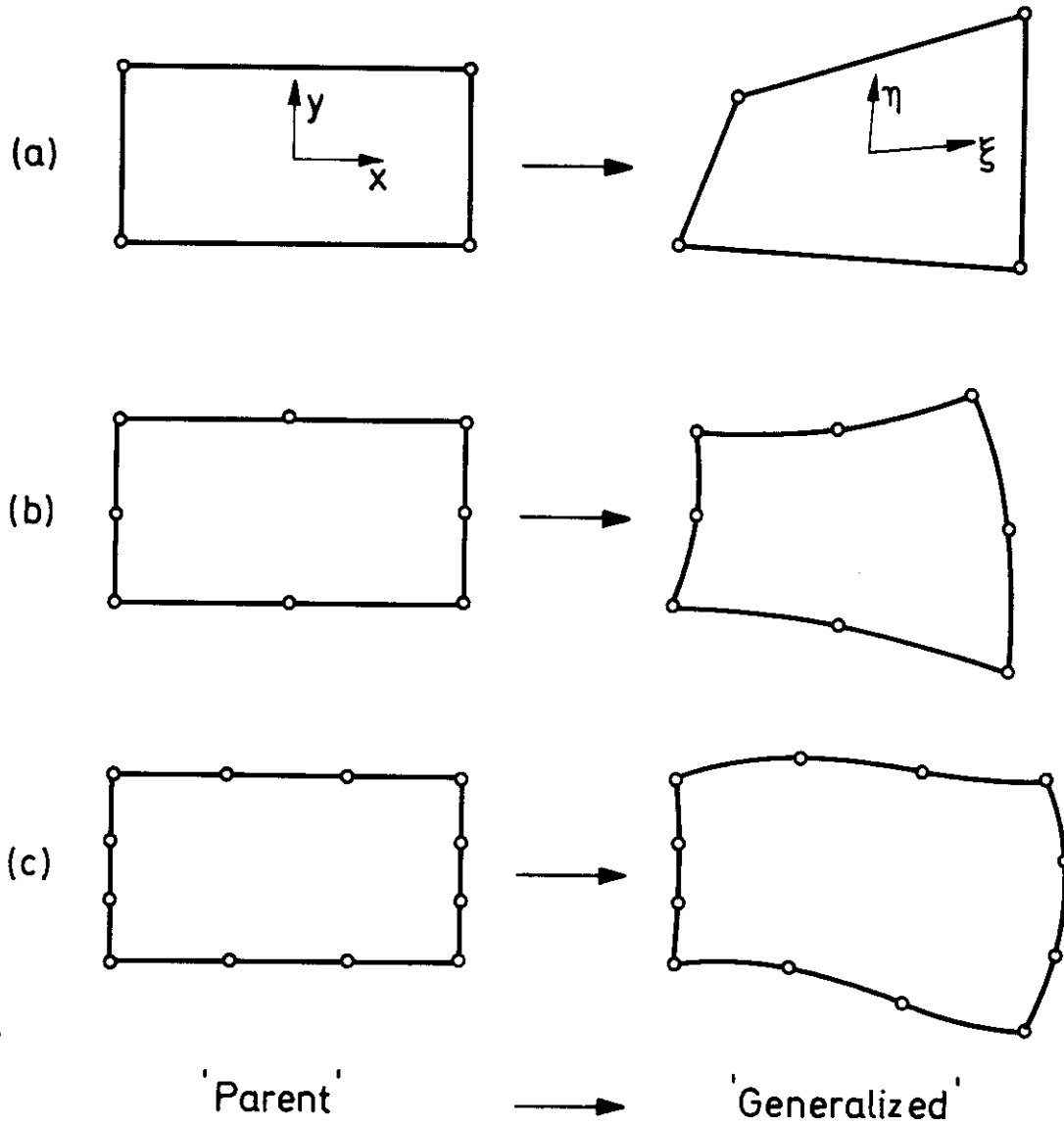


Figure 1. Two Dimensional, Quadrilateral, Family

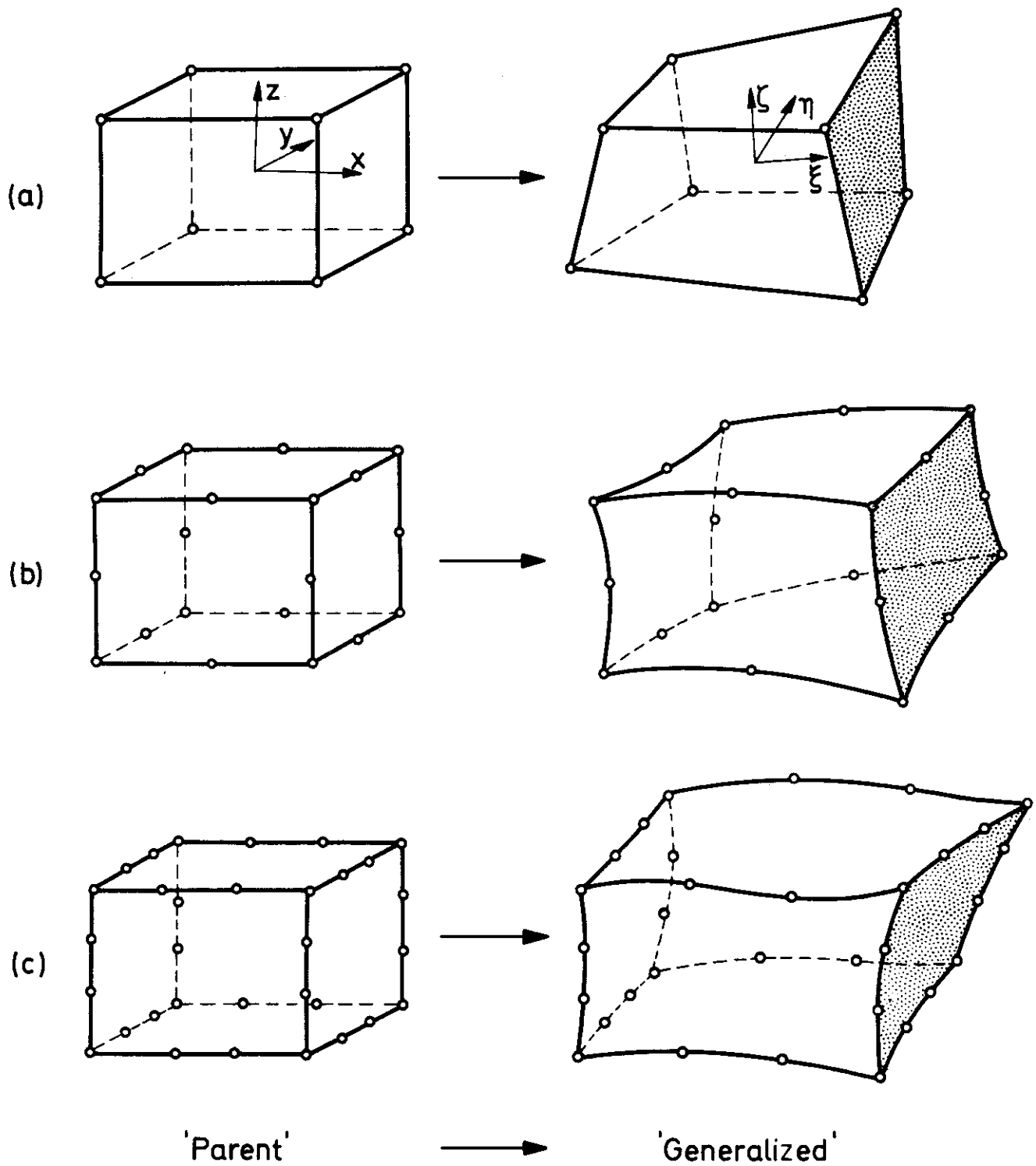


Figure 2. Three Dimensional, Hexahedron, Family

These new elements are not strictly 'isoparametric' according to the definitions of Reference 3. Nevertheless conformity between elements is maintained, and rigid body modes and constant strain criteria are in turn exactly and approximately satisfied.

SECTION II

COORDINATE SYSTEM FOR AN AXISYMMETRIC ELEMENT

Consider a system of curvilinear coordinates $\xi - \eta$ defined inside the element shown in Figure 3a, with typical node pairs i_{top} and i_{bottom} . The 'normal' direction η as defined by such points is in general only approximately normal to the mid-surface. However, it is in this direction η that the linearity constraint is imposed.

The coordinates r and z within the element are linked with the curvilinear coordinates by the relation

$$\begin{bmatrix} r \\ z \end{bmatrix} = \sum N_i \frac{(1 + \eta)}{2} \begin{bmatrix} r_i \\ z_i \end{bmatrix}_{\text{top}} + \sum N_i \frac{(1 - \eta)}{2} \begin{bmatrix} r_i \\ z_i \end{bmatrix}_{\text{bottom}} \quad (1)$$

Where N_i is a shape function in ξ only. The element extends from ξ and $\eta = -1$ to 1 in the usual manner (Reference 3).

This can also be written in terms of the mid-surface coordinates and the angle of the 'normal' ϕ_i shown in Figure 3b as follows:

$$\begin{bmatrix} r \\ z \end{bmatrix} = \sum N_i \begin{bmatrix} r_i \\ z_i \end{bmatrix}_{\text{mid}} + \sum N_i \eta \frac{t_i}{2} \begin{bmatrix} \cos \phi_i \\ \sin \phi_i \end{bmatrix} \quad (2)$$

where t_i is the scalar length of the normal.

It is convenient to use linear functions N_i for elements defined by two nodes, parabolic functions for three nodes and so on as shown in Figure 4, so that middle surfaces of elements become linear, parabolic, cubic. Typical shape functions are

Linear Linear
$$N_i = \frac{1}{2} (1 + \xi_0) \quad (3)$$

Where $\xi_0 = \xi \xi_i$ and $\xi_i = \pm 1$

Quadratic For an end node

$$N_i = \frac{1}{2} (1 + \xi_0) \xi_0 \quad (4)$$

and for a midside node

$$N_i = (1 - \xi^2) \quad (5)$$

Cubic For an end node

$$N_i = \frac{1}{16} (1 + \xi_0) (-1 + 9\xi^2) \quad (6)$$

and for a node with $\xi_i = \pm \frac{1}{3}$

$$N_i = \frac{9}{16} (1 - \xi^2) (1 + 9\xi_0) \quad (7)$$

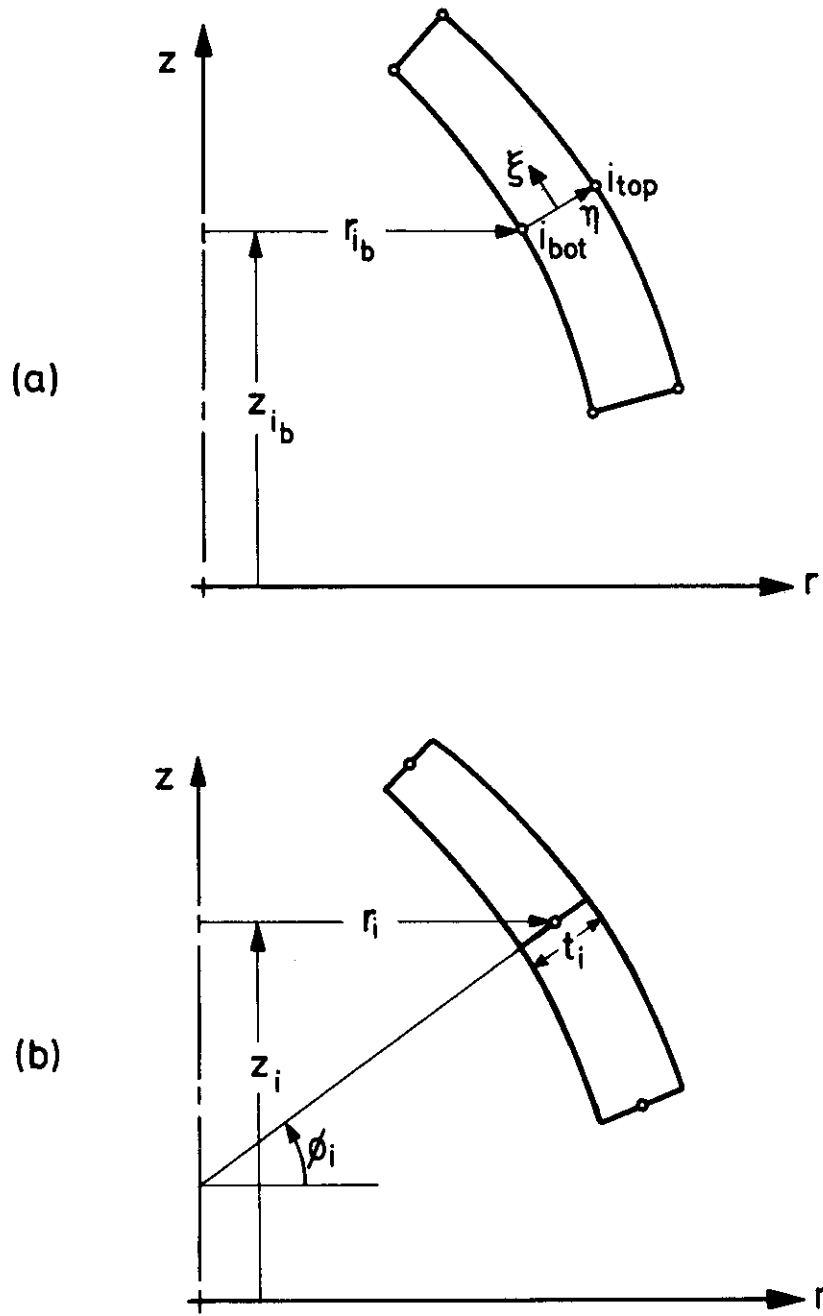


Figure 3. Coordinates for an Axisymmetric Shell Problem

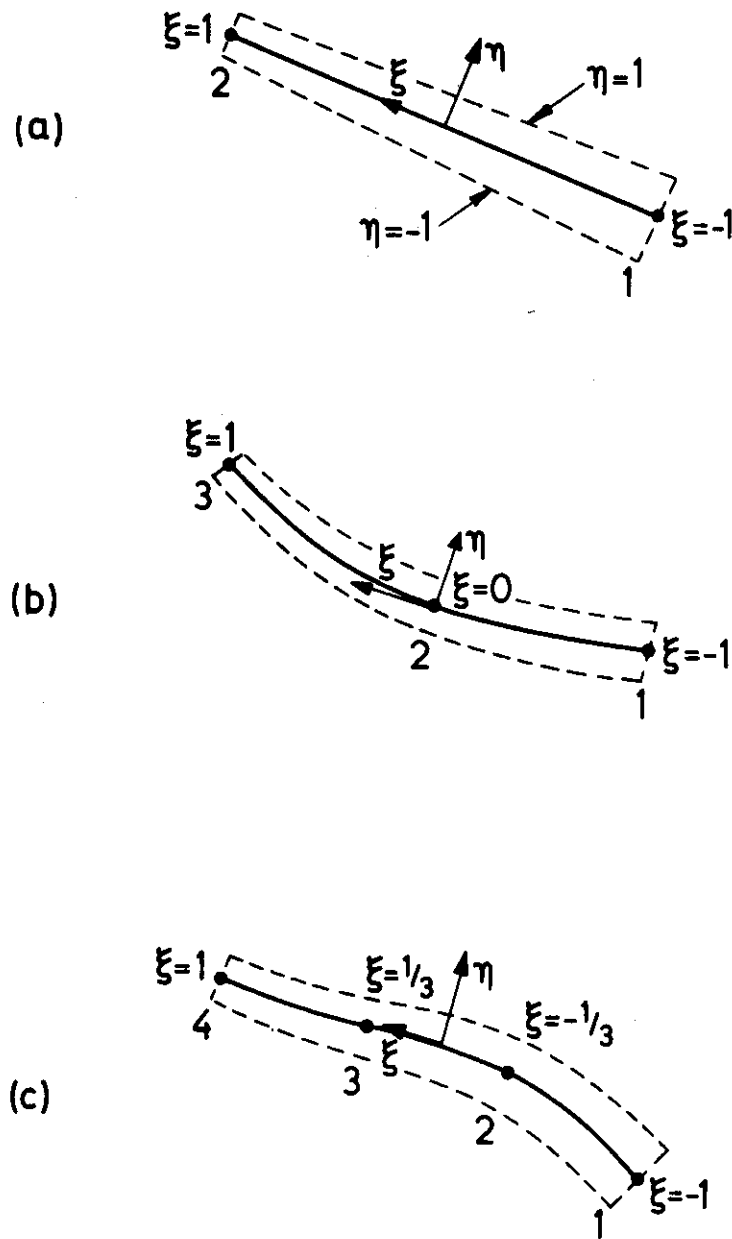


Figure 4. Linear (a), Parabolic (b) and Cubic (c) Shell Elements

SECTION III
DISPLACEMENT PATTERN OF AN AXISYMMETRIC
ELEMENT UNDER AXISYMMETRIC LOADING

Assuming that the 'normals' are straight and non-extensible, the general displacements (u, v) are defined by the displacements of the mid-surface nodes in the r - z directions and the rotation of the normal at such nodes (u_i, v_i and α_i of Figure 5). Within the element the displacements thus defined are

$$\begin{bmatrix} u \\ v \end{bmatrix} = \sum N_i \begin{bmatrix} u_i \\ v_i \end{bmatrix} + \sum N_i \eta \frac{t_i}{2} \begin{bmatrix} -\sin \phi_i \\ \cos \phi_i \end{bmatrix} \alpha_i \quad (8)$$

Comparison with Expression 2 shows that the isoparametric concept is retained only in the ξ direction.

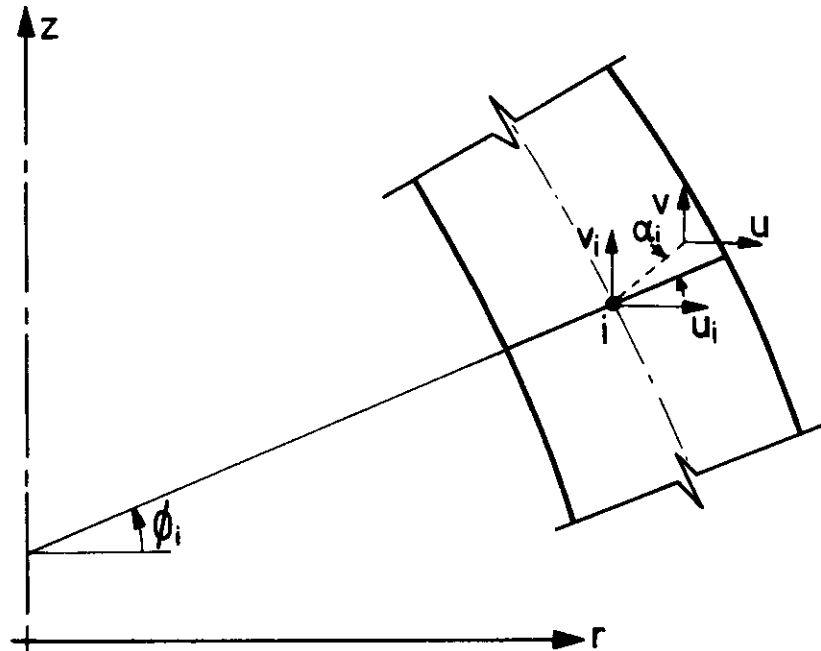


Figure 5. 'Global' Displacements in an Axisymmetric Shell

SECTION IV
EVALUATION OF ELEMENT CHARACTERISTICS
FOR AXISYMMETRIC PROBLEMS

Element characteristics such as stiffness matrices etc., can now be determined in the usual manner. For example, the stiffness matrix is defined as

$$[k]^e = \int_{Vol.} [B]^T [D] [B] d(Vol) \quad (9)$$

where the $[B]$ matrix relates the local strains $\{\epsilon\}$ to the nodal displacements

$$\{\epsilon\} = [B] \{\delta\}^e \quad (10)$$

using the notation of the finite element text (Reference 7).

However, it is necessary to avoid the spurious side-effects of inextensibility by assuming a zero modulus in the true normal direction. The local strains must therefore be defined in appropriate directions.

Consider local orthogonal coordinates, z' parallel to a surface $\eta = \text{constant}$ within the shell, and r' created truly normal to this, with the corresponding displacement components v' and u' as shown in Figure 6. The strains in these local coordinates are given by

$$\{\epsilon'\} = \begin{bmatrix} \epsilon'_z \\ \epsilon_\theta \\ \gamma_{r'z'} \end{bmatrix} = \begin{bmatrix} \frac{\partial v'}{\partial z'} \\ \frac{u}{r} \\ \frac{\partial v'}{\partial r'} + \frac{\partial u'}{\partial z'} \end{bmatrix} \quad (11)$$

neglecting the strain normal to the surface in accordance with our shell assumptions, and writing the hoop strain directly in global coordinates.

It is now necessary to write these strains in terms of the nodal displacements and the local coordinates ξ, η . By Equations 2 and 8 the second term is directly available; but two transformations are needed to obtain the others. These are easily derived.

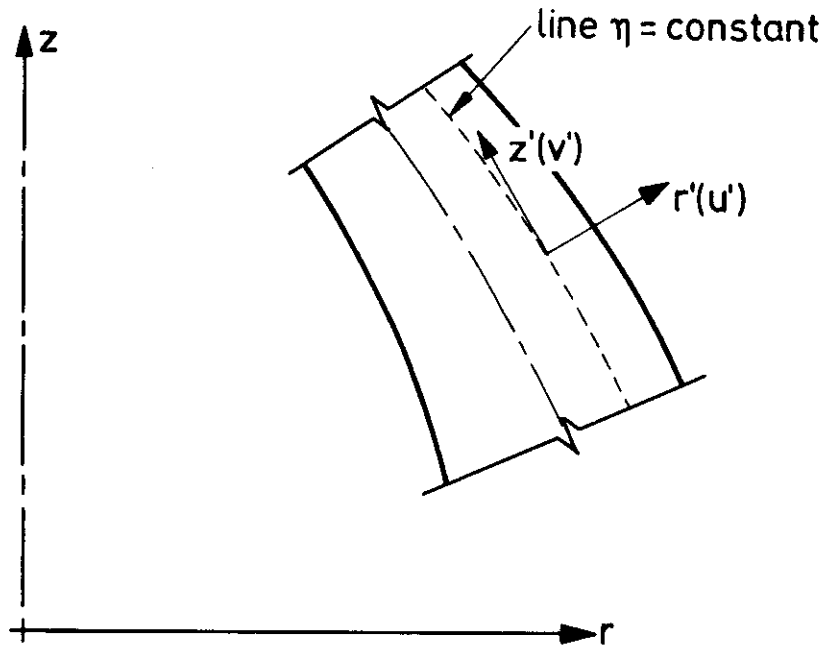


Figure 6. Local Orthogonal Coordinates for Symmetric Loading

Firstly, the r, z derivatives of u, v are derived from their ξ, η derivatives. This process is well known and gives

$$\begin{bmatrix} \frac{\partial v}{\partial z} & \frac{\partial u}{\partial z} \\ \frac{\partial v}{\partial r} & \frac{\partial u}{\partial r} \end{bmatrix} = [J]^{-1} \begin{bmatrix} \frac{\partial v}{\partial \xi} & \frac{\partial u}{\partial \xi} \\ \frac{\partial v}{\partial \eta} & \frac{\partial u}{\partial \eta} \end{bmatrix} \quad (12)$$

with the Jacobian matrix $[J]$ defined as

$$[J] = \begin{bmatrix} \frac{\partial z}{\partial \xi} & \frac{\partial r}{\partial \xi} \\ \frac{\partial z}{\partial \eta} & \frac{\partial r}{\partial \eta} \end{bmatrix} \quad (13)$$

Secondly, changing to local orthogonal coordinates one can write

$$\begin{bmatrix} \frac{\partial v'}{\partial z'} & \frac{\partial u'}{\partial z'} \\ \frac{\partial v'}{\partial r'} & \frac{\partial u'}{\partial r'} \end{bmatrix} = [\theta]^T \begin{bmatrix} \frac{\partial v}{\partial z} & \frac{\partial u}{\partial z} \\ \frac{\partial v}{\partial r} & \frac{\partial u}{\partial r} \end{bmatrix} [\theta] \quad (14)$$

where $[\theta]$ is the matrix of direction cosines of the z' and r' axes. Parametrically these can be obtained at any value of ξ and η , noting that directions z' and ξ coincide, as

$$[\theta] = \frac{1}{\sqrt{\left(\frac{\partial z}{\partial \xi}\right)^2 + \left(\frac{\partial r}{\partial \xi}\right)^2}} \begin{bmatrix} \frac{\partial z}{\partial \xi} & -\frac{\partial r}{\partial \xi} \\ \frac{\partial r}{\partial \xi} & \frac{\partial z}{\partial \xi} \end{bmatrix} \quad (15)$$

In this, all the derivatives are obtained numerically from Equation 2.

The $[B']$ matrix, which defines the local strains in terms of the nodal displacements, can now be evaluated at any point within the element.

$$\{\epsilon'\} = [B'] \begin{bmatrix} u_1 \\ v_1 \\ \alpha_1 \\ \vdots \\ u_i \\ v_i \\ \alpha_i \\ \vdots \end{bmatrix} = [B'] \{\delta\}^e \quad (16)$$

The corresponding elasticity matrix $[D']$ is now easily written. In an isotropic case for instance it is

$$[D'] = \frac{E}{1-\nu^2} \begin{bmatrix} 1 & \nu & 0 \\ \nu & 1 & 0 \\ 0 & 0 & \frac{1-\nu}{2k} \end{bmatrix} \quad (17)$$

Where E and ν are the elastic modulus and Poisson's ratio respectively. The factor k is included to account more accurately for shear strain energy. As the displacements vary linearly across the thickness of the shell, the shear stresses are sensibly constant. However, they are known to be approximately parabolic, and the factor $k = 1.2$ is included to improve the representation (see standard strength of materials theory of shear deformation energy).

The final step is to define the volume element for the integrations, such as that in the stiffness matrix of Equation 9. This again is standard; for an annular element it becomes

$$d(\text{vol}) = 2\pi r (\det [J] d\xi d\eta) \quad (18)$$

The actual integration is carried out numerically within the simple limits of ± 1 , using several Gauss points as described in References 1 to 3. Only two Gauss points are needed in the η (thickness) direction, and 3 or 4 in the ξ direction, depending on whether the elements are parabolic or cubic.

Either Equation 1 or 2 can be used to define the element geometry in the program. For very thick shells Equation 1 may be preferable, but for thinner shells, particularly if branching occurs, the thickness slope definition is better.

SECTION V EXTENSION TO NON-SYMMETRIC LOADING

It is now well known that nonsymmetric loads acting on axisymmetric bodies can be treated separately for each harmonic, using Fourier analysis, because their effects are uncoupled (References 8, 9, and 10). Thus, if the radial, axial and tangential loads are given by

$$\begin{bmatrix} R \\ Z \\ T \end{bmatrix} = \begin{bmatrix} R_n \cos n\theta \\ Z_n \cos n\theta \\ T_n \sin n\theta \end{bmatrix} \quad (19)$$

then the resulting displacements are given by

$$\begin{bmatrix} u \\ v \\ w \end{bmatrix} = \begin{bmatrix} u_n \cos n\theta \\ v_n \cos n\theta \\ w_n \sin n\theta \end{bmatrix} \quad (20)$$

By considering the amplitudes of the displacement, the appropriate stiffness matrices can be found by a volume integration which includes the θ variations.

To extend the axisymmetric analysis in this way, we must add one further degree of freedom w to the general displacement in Equation 8, and two further degrees of freedom at each nodal normal, (one displacement and one rotation) giving five altogether.

Assuming the loading is as given by Equation 19 and retaining the assumptions used previously in deriving the displacement pattern, we can write in place of Equation 8

$$\begin{bmatrix} u \\ v \\ w \end{bmatrix} = \begin{bmatrix} \cos n\theta & 0 & 0 \\ 0 & \cos n\theta & 0 \\ 0 & 0 & \sin n\theta \end{bmatrix} \left(\sum N_i \begin{bmatrix} u_i \\ v_i \\ w_i \end{bmatrix} + \sum N_i \eta \frac{t_i}{2} \begin{bmatrix} -\sin \phi_i & 0 \\ \cos \phi_i & 0 \\ 0 & 1 \end{bmatrix} \begin{bmatrix} \alpha_i \\ \beta_i \end{bmatrix} \right) \quad (21)$$

where β_i is the rotation of the 'nodal normal' in the circumferential direction. The strains are now defined in terms of global coordinates and displacements as

$$\{\epsilon\} = \begin{bmatrix} \epsilon_r \\ \epsilon_z \\ \epsilon_\theta \\ \gamma_{rz} \\ \gamma_{r\theta} \\ \gamma_{z\theta} \end{bmatrix} = \begin{bmatrix} \frac{\partial u}{\partial r} \\ \frac{\partial v}{\partial z} \\ \frac{u}{r} + \frac{\partial w}{r \partial \theta} \\ \frac{\partial u}{\partial z} + \frac{\partial v}{\partial r} \\ \frac{\partial u}{r \partial \theta} + \frac{\partial w}{\partial r} - \frac{w}{r} \\ \frac{\partial w}{\partial z} + \frac{\partial v}{r \partial \theta} \end{bmatrix} \quad (22)$$

By a transformation similar to Equation 12, these strains can be determined explicitly in terms of ξ , η and θ coordinates, using the Jacobian matrix $[J]$.

The strains in the directions of the local set of axes, one of which is normal to line $\eta = \text{constant}$ and the other tangential as shown in Figure 7 are obtained by a transformation similar to Equation 14.

$$\begin{bmatrix} \epsilon'_z & \frac{1}{2} \gamma'_{z'r'} & \frac{1}{2} \gamma'_{z'\theta} \\ \frac{1}{2} \gamma'_{z'r'} & \epsilon'_r & \frac{1}{2} \gamma'_{r'\theta} \\ \frac{1}{2} \gamma'_{z'\theta} & \frac{1}{2} \gamma'_{r'\theta} & \epsilon'_\theta \end{bmatrix} = [\theta]^T \begin{bmatrix} \epsilon_z & \frac{1}{2} \gamma_{zr} & \frac{1}{2} \gamma_{z\theta} \\ \frac{1}{2} \gamma_{zr} & \epsilon_r & \frac{1}{2} \gamma_{r\theta} \\ \frac{1}{2} \gamma_{z\theta} & \frac{1}{2} \gamma_{r\theta} & \epsilon_\theta \end{bmatrix} [\theta] \quad (23)$$

where again the matrix $[\theta]$ consists of appropriate direction cosines between the axes (3 x 3). Thus the $[\theta]$ of Equation 15 occurs, together with unity, because the circumferential axis is unchanged.

The vector $\{\epsilon\}$ is found directly from Equation 23, and the calculation proceeds as before.

Again neglecting the 'thickness' direction, the $[D']$ matrix for an isotropic material now becomes

$$[D'] = \frac{E}{1-\nu^2} \begin{bmatrix} 1 & \nu & 0 & 0 & 0 \\ \nu & 1 & 0 & 0 & 0 \\ 0 & 0 & \frac{1-\nu}{2k} & 0 & 0 \\ 0 & 0 & 0 & \frac{1-\nu}{2k} & 0 \\ 0 & 0 & 0 & 0 & \frac{1-\nu}{2} \end{bmatrix} \quad (24)$$

Clearly the correction factor $k = 1.2$ must not be included in the last term, which refers to a shear strain component $z'\theta$ in the plane of the shell.

SECTION VI

A GENERAL CURVED SHELL ELEMENT

The preceding sections describe in some detail the process of degeneration, as it applies to basically two dimensional elements. As mentioned in the introduction, essentially the same procedure can be adopted in fully three-dimensional elements, giving a general curved thick shell element of arbitrary shape as shown in Figure 8.

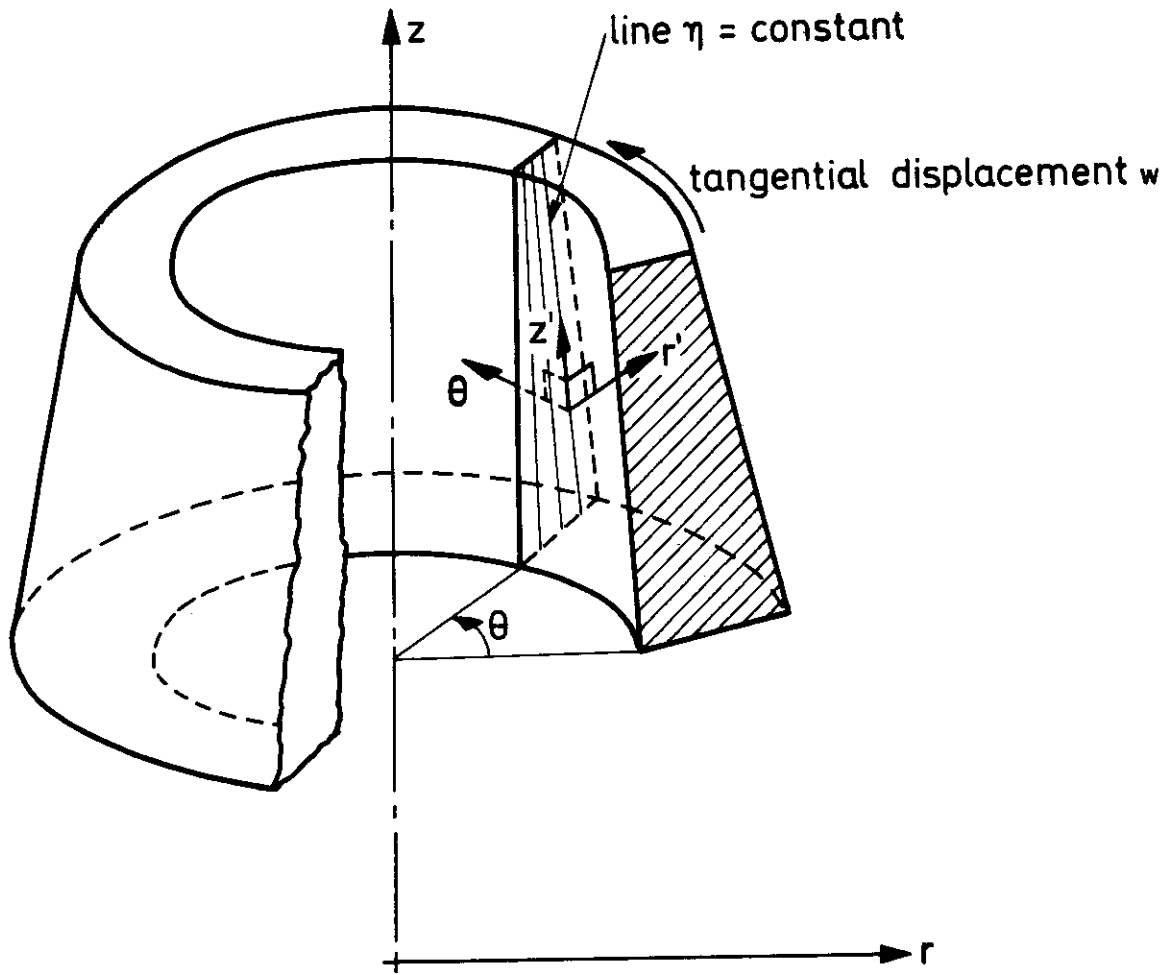


Figure 7. Local Orthogonal Coordinates for Nonsymmetric Loading

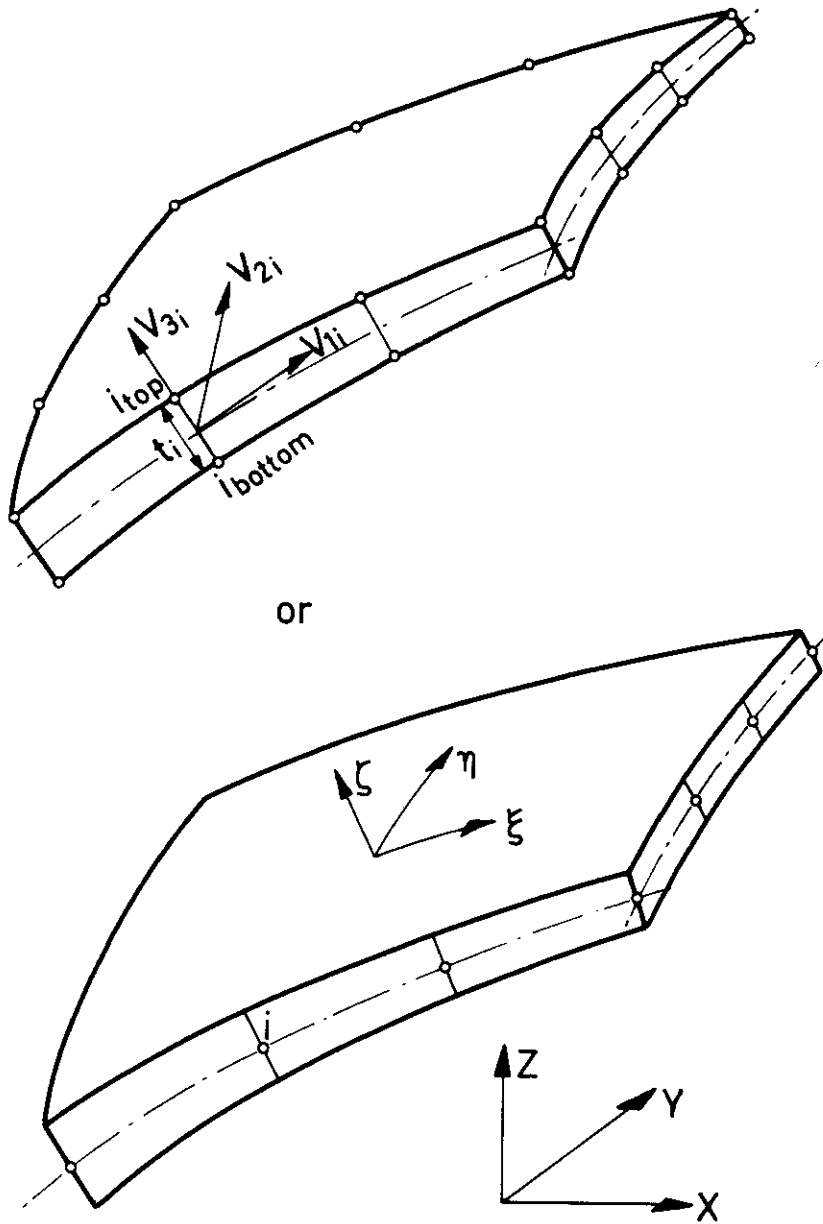


Figure 8. A General Curved Shell Element

Once again the coordinates of the top and bottom points associated with a node defines the coordinate within the thickness of the shell and the directions of the 'normal' before distortion.

The element curvilinear coordinates are related to the global x, y, z system by a relationship similar to that given by Equation 1

$$\begin{bmatrix} x \\ y \\ z \end{bmatrix} = \sum N_i \frac{(1 + \zeta)}{2} \begin{bmatrix} x_i \\ y_i \\ z_i \end{bmatrix}_{\text{top}} + \sum N_i \frac{(1 - \zeta)}{2} \begin{bmatrix} x_i \\ y_i \\ z_i \end{bmatrix}_{\text{bottom}} \quad (25)$$

in which however the N_i are shape functions, now given in terms of ξ and η i.e.

$$N_i = N_i (\xi, \eta) \quad (26)$$

Once again linear, parabolic, cubic etc. shapes can be adopted for a middle surface and suitable shape functions generated. These are as used in Reference 3 for two-dimensional analysis and are not given here explicitly.

The displacement pattern has now to be assumed, and it is slightly more complex than one might expect from Equation 8, as two rotations of the 'normal' about axes orthogonal to it have to be determined.

If \hat{v}_{3i} represents a unit vector in the direction of the nodal 'normal', and if \hat{v}_{1i} and \hat{v}_{2i} are unit orthogonal vectors, then we can write for the displacements in global axes x, y, z

$$\begin{bmatrix} u \\ v \\ w \end{bmatrix} = \sum N_i \begin{bmatrix} u_i \\ v_i \\ w_i \end{bmatrix} + \sum N_i \zeta \frac{t_i}{2} \begin{bmatrix} \hat{v}_{1i} & \hat{v}_{2i} \end{bmatrix} \begin{bmatrix} \alpha_i \\ \beta_i \end{bmatrix} \quad (27)$$

where u_i, v_i, w_i are the displacements at the midsurface node, and α_i, β_i are the two rotations about directions \hat{v}_{2i} and $-\hat{v}_{1i}$ respectively.

An infinity of systems of cartesian axes exist which include the specified \hat{v}_{3i} , and a consistent definition giving unique axes must be adopted. In general, of course, the vectors \hat{v}_{1i} and \hat{v}_{2i} are only approximately tangent to the mid-surface.

Having defined the displacements we can obtain the global strains, and transform them into a set of orthogonal directions two of which lie tangent to the surface $\zeta = \text{constant}$. This new set of directions must not be confused with the previous approximate 'normal' set. Transformations follow the pattern of Section III, but are not given here in detail; the reader should consult a separate paper (Reference 11). In this connection it should be remarked that considerable utilization was made of the matrix vector comprehensive subroutine scheme.

SECTION VII
CURVED MEMBRANE ELEMENTS

To cover the full range of shell thickness, and occasionally for other purposes (when treating thin linings attached to solid elements), one needs elements which present no resistance to bending. If a shell is very thin indeed, the strains must be sensibly constant through its thickness, and equal to those at its midsurface.

Immediately it follows that displacements for the general membrane element become simply

$$\begin{bmatrix} u \\ v \\ w \end{bmatrix} = \sum N_i \begin{bmatrix} u_i \\ v_i \\ w_i \end{bmatrix} \quad (28)$$

without the rotations of the normals being considered, so that the degrees of freedom reduce to only three direct displacements per node; thus the membrane element is perfectly isoparametric and retains all the properties (Reference 3). The remaining details of the transformation follow the standard pattern described in Section V. Only three in-plane strains, two tensions and the in-plane shear, contribute now to the stiffness matrix.

In the same way axisymmetric membrane elements are easily formulated, for example by removing the rotation term from Equation 8.

SECTION VIII

SOME AXISYMMETRIC EXAMPLES

The first example is designed to test the accuracy of the new elements when dealing with very thick shells. A simple Lamé cylinder under internal pressure is considered and some results for hoop stresses shown in Figure 9.a. Only one element is used in solution (and obviously it does not matter whether it is linear, parabolic or cubic). With extreme thickness to internal radius ratio of one the linear distribution of stresses fits almost the best approximation to the Lamé curve. For larger radius-thickness ratios the finite element results are indistinguishable from the exact solution.

In Figure 9.b a similar problem of a thick sphere is dealt with. Here one cubic element is again used and it is remarkable how well this representation approximates to the geometry and to the final results.

The second example deals with the classical Timoshenko (Reference 12) solution of a spherical cap, Figure 10. Geometrical details are shown there and with a finite thickness the distinction made between loading being applied to outer (Case I) or inner (Case II) surfaces. The average stress resultants reproduce almost exactly the theoretical curve using a division of 24 cubic-type elements, but it is of interest to note the differences arising between the two loading cases.

Figure 11 shows the same problem solved for a thicker shell ($t = 9''$). Results are compared with a full two-dimensional solution of type indicated in References 3 and 13. The computer times necessary for equivalent solutions here were in the ratio of 1 : 3.

The third example deals with a very thin restrained pipe (Figure 12) which has also been previously solved by finite element methods by Grafton and Strome (Reference 8) and Percy et al (Reference 9). Here the effect of various subdivisions into cubic elements is studied. Even with two elements the displacement pattern is well reproduced but six elements were needed to obtain reasonable stress predictions. For solution of the same problem in Reference 9, a much larger number of elements was needed even to obtain displacement patterns.

The last example concerns another test example now of an axisymmetric tube under nonsymmetric, harmonic loads. Here the problem and the results for several harmonics as given in Figure 13 and are compared with results of Percy et al (Reference 9) as well as those of Budiansky and Radkowski (Reference 14).

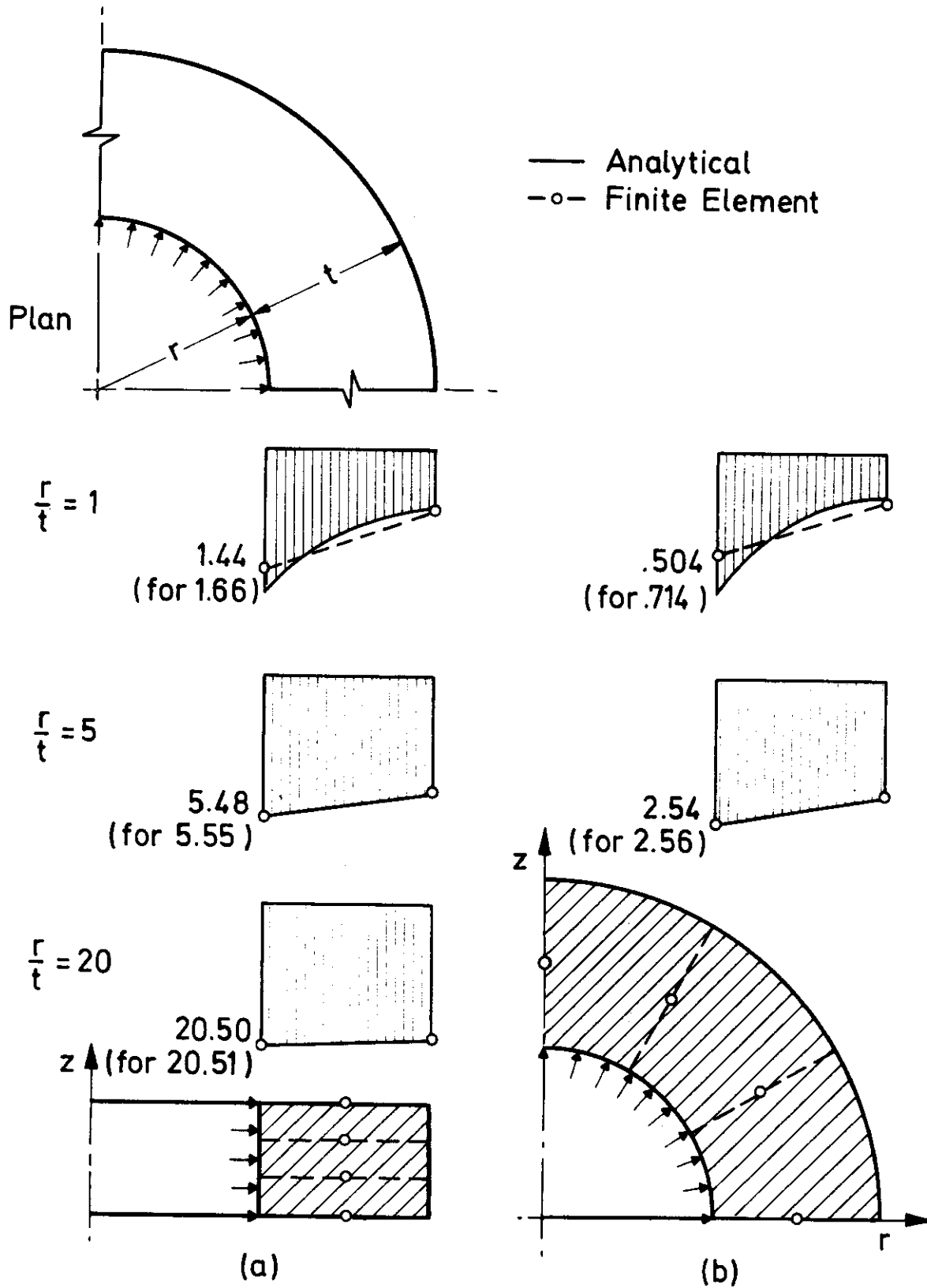


Figure 9. Lamé Solution for Hoop Stresses (a) Cylinder Under Uniform Internal Pressure (b) Sphere Under Uniform Internal Pressure

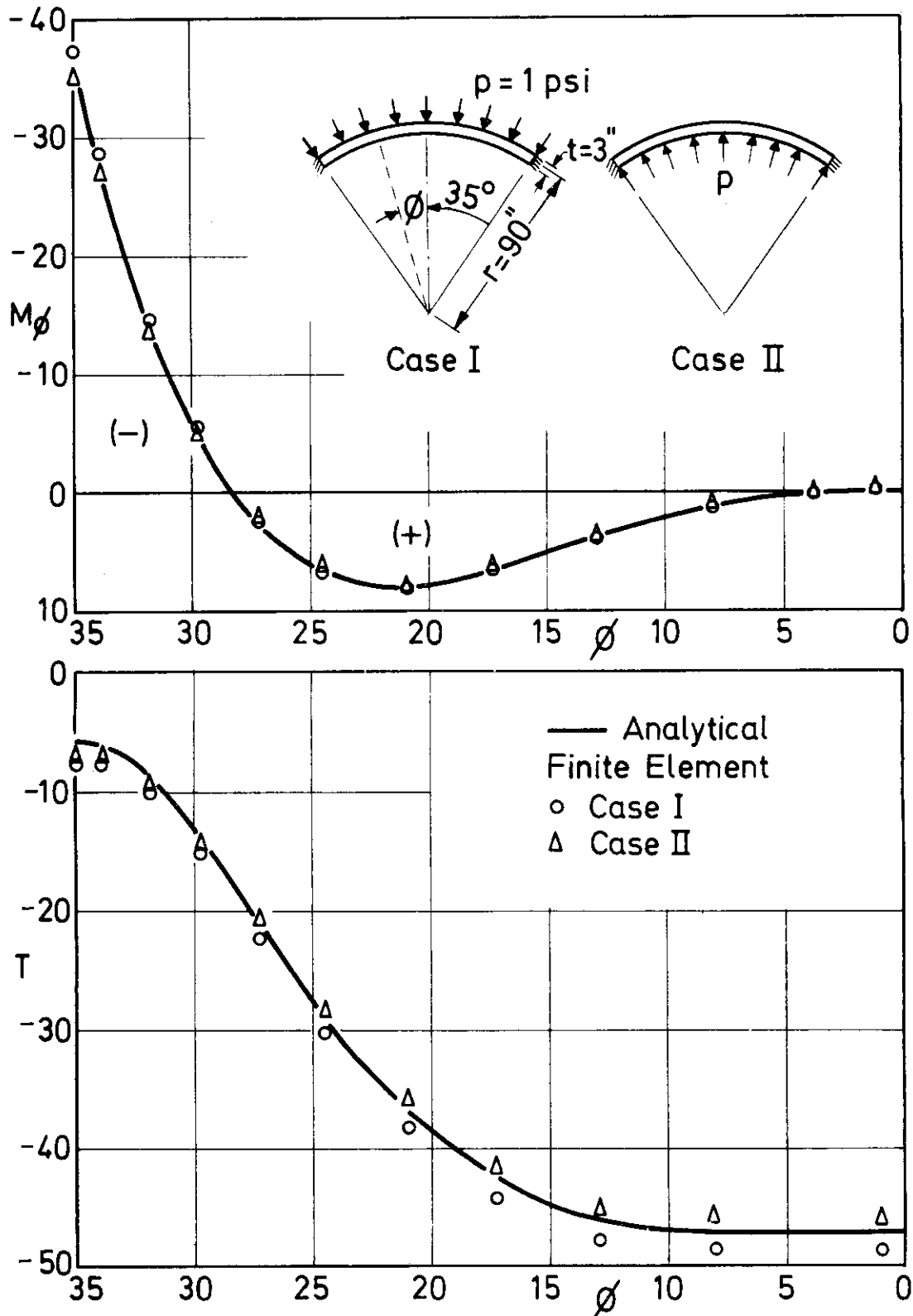


Figure 10. Spherical Shell Under Uniform Pressure. Analysed With 24 Elements in A.P. (1st Element Subtends an Angle of .1 Degree From the Fixed End). M_ϕ = Meridional Bending Moment, in-lb/in., T = Hoop Forces, lb/in., $\nu = 1/6$.

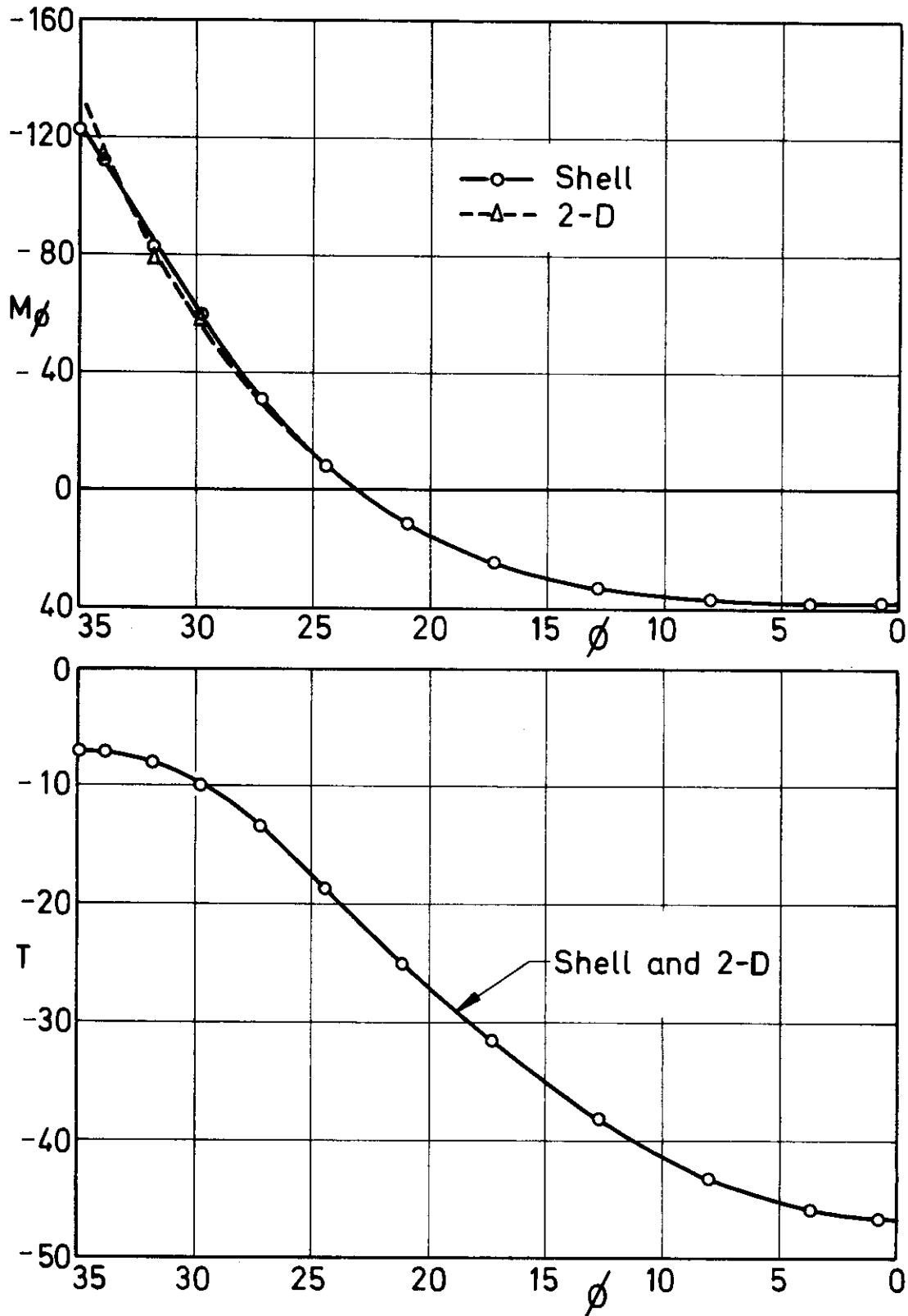


Figure 11. Problem of Figure 10 Case I With Shell Thickness of 9 Ins.

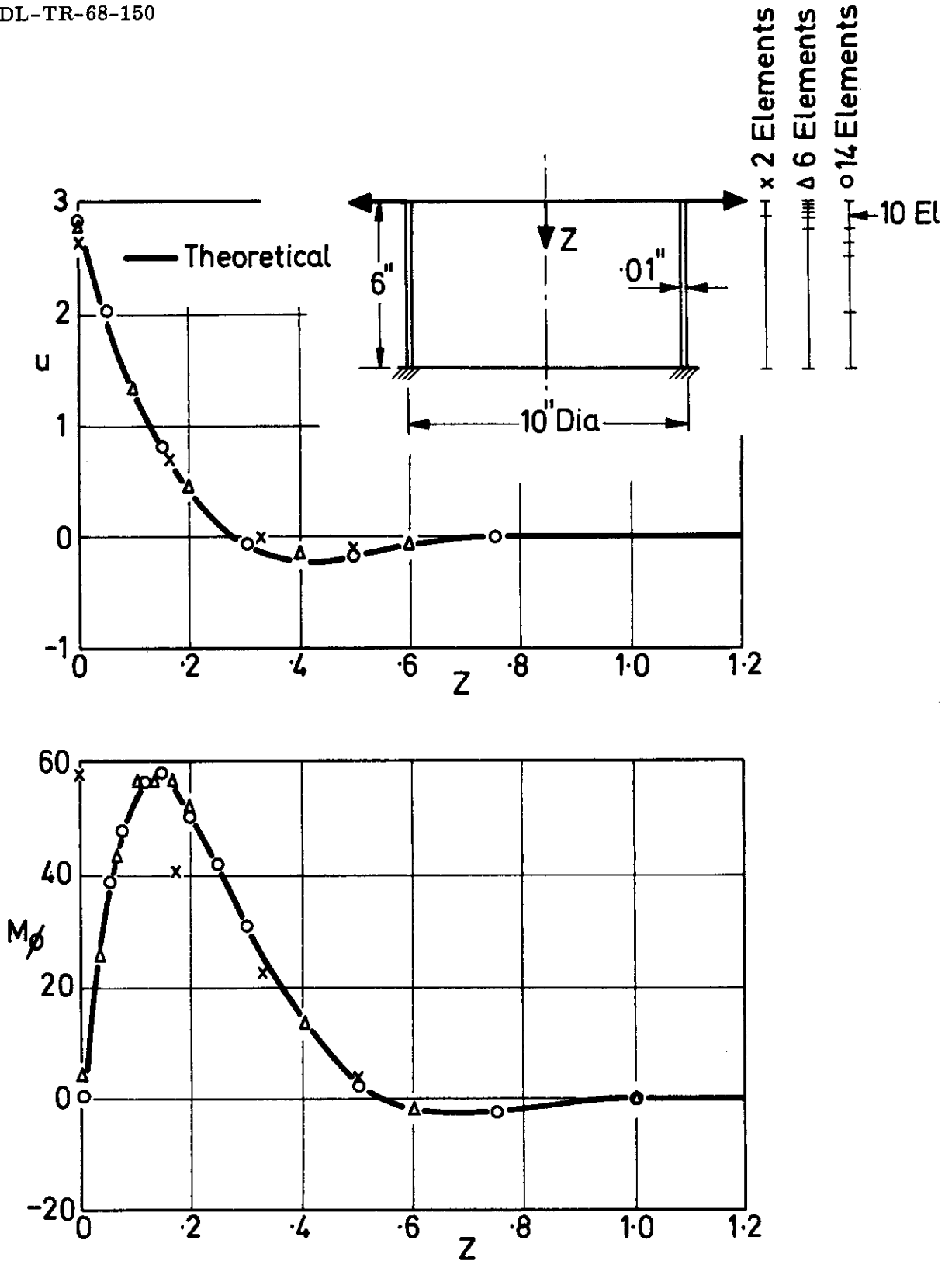


Figure 12. Cylindrical Clamped Shell Under Radial Edge Load, u = Radial Displacements, in. $\times 10^{-3}$, M_ϕ = Meridional Moments, in-lb/in. $\times 10^{-3}$, $E = 10^7 \text{ lb/in}^2$, $\nu = 0.3$.

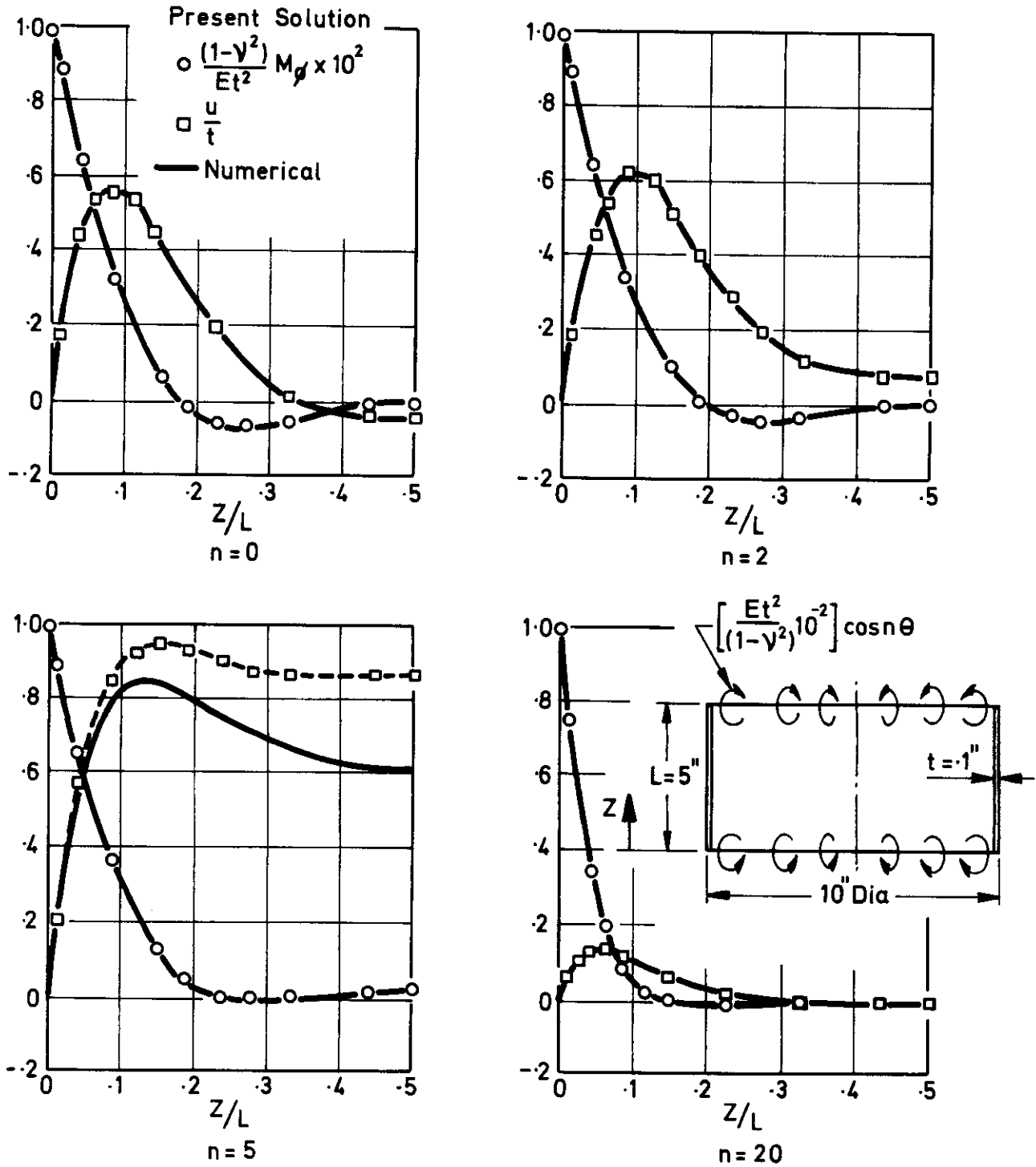


Figure 13. Cylinder Under Harmonic Edge Couples. Finite Element and Numerical Results of References 9 and 14 (Solid Line) Compared With Present Solution. Analyzed Half With 15 Elements in A. P. (1st Element is 0.02 From the End). M_ϕ = Meridional Bending Moment (Amplitude) u = Radial Deflection (Amplitude), $E = 1$, $\nu = 0.3$.

The general agreement of displacements and moments is excellent with exception of the displacement results for the fifth harmonic. This discrepancy remains somewhat puzzling since a full two-dimensional analysis (Reference 13) of the same problem also differs at the same point.

SECTION IX

SOME ARBITRARY THICK SHELL SOLUTIONS

The first problem is that of a circular ring line supported at the base under the action of gravity, Figure 14. Results agree well with those predicted by simple engineers' bending theory.

A more complex situation is illustrated for a variable thickness tube, supported at two points as in Figures 15 and 16. Again the loading is that due to self weight.

The last example is that of a fairly thick shell representing an arch dam of symmetric shape. Figure 17 shows the general division into nine thick shell elements.

In Figure 18 the downstream displacement plot is compared with results of a complete three-dimensional solution of this problem (Reference 4). The results agree very well though it must be mentioned that a slight difference in the manner of load application existed between the two solutions.

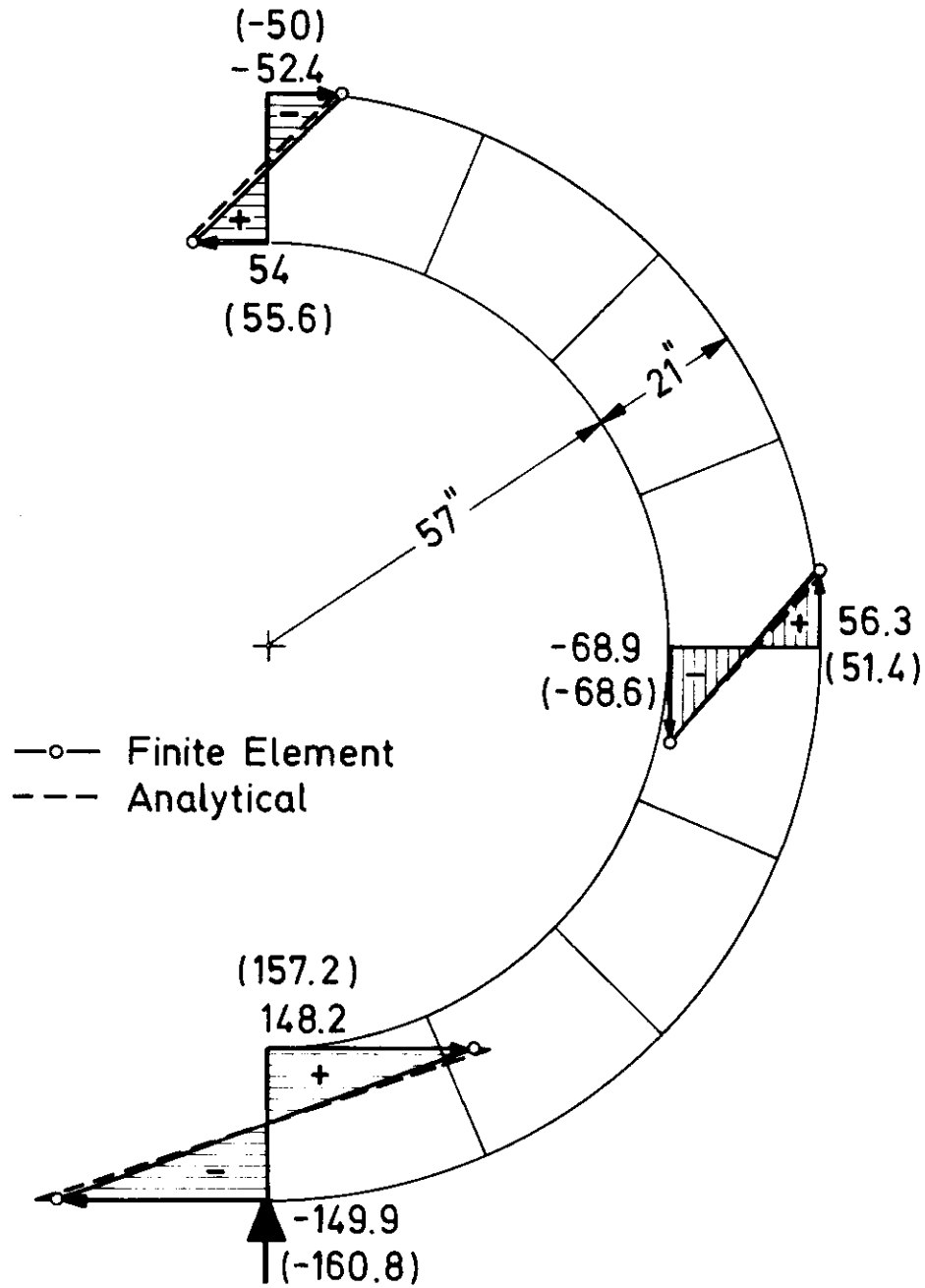


Figure 14. A Thick Circular Ring Under Action of Gravity With Line Support. Analyzed With 8 Parabolic Elements. $E = 3 \times 10^6 \text{ lb/in.}^2$, $\nu = 0.15$, $\gamma = 140 \text{ lb/ft}^3$.

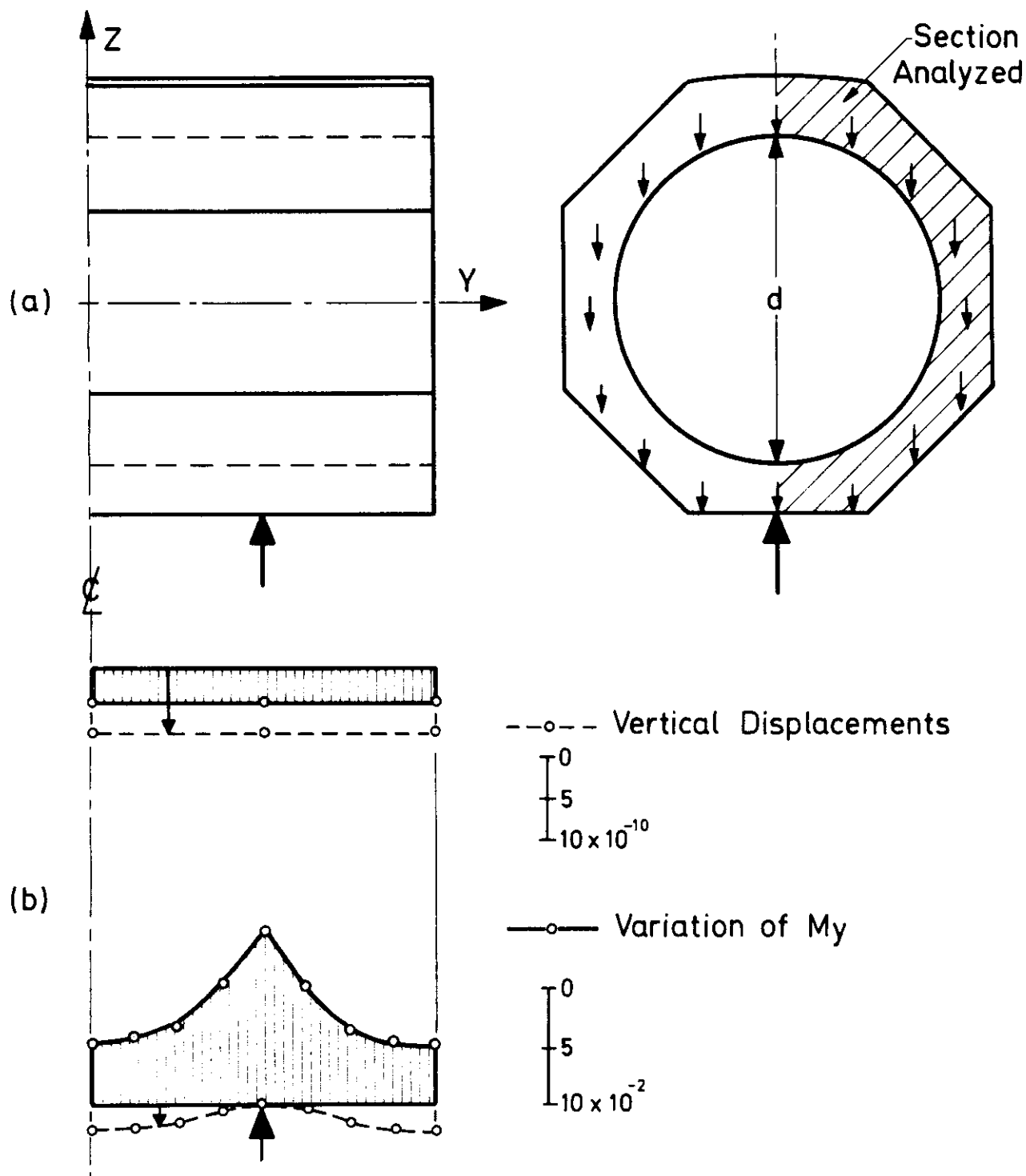


Figure 15. A Variable Thickness Conduit Supported at Two Points Under Action of Gravity. Analyzed With 32 Parabolic Elements (4 x 8 Mesh).
 (a) Geometry (b) Variation of Displacements $w/\gamma d^4$ and Axial Bending Moments $M_y/\gamma d^3$ Along Top and Bottom Axes.

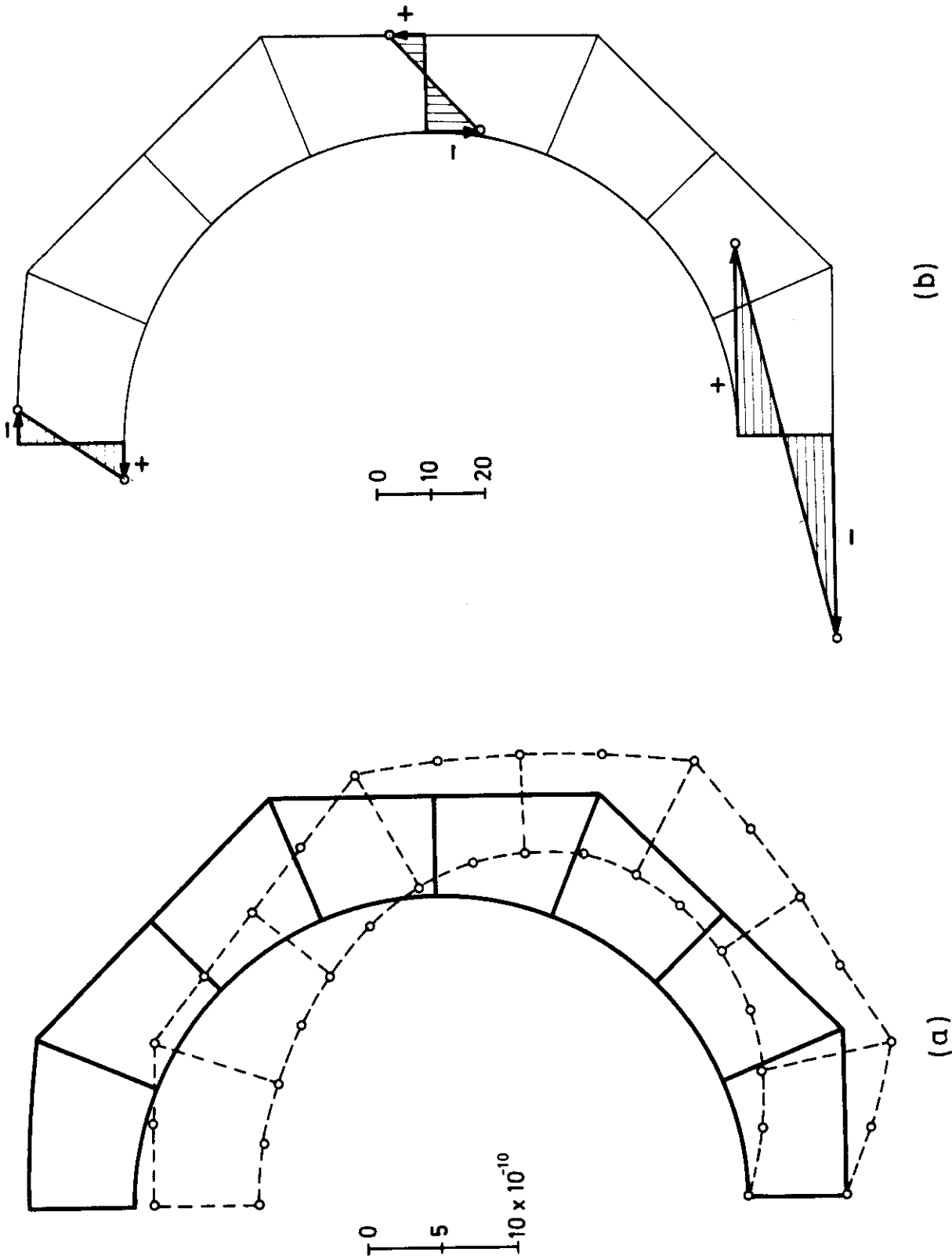


Figure 16. Problem of Figure 15: (a) Distortion of Support Section (b) Hoop Stresses $\sigma_{\theta} / \gamma d$

Controls

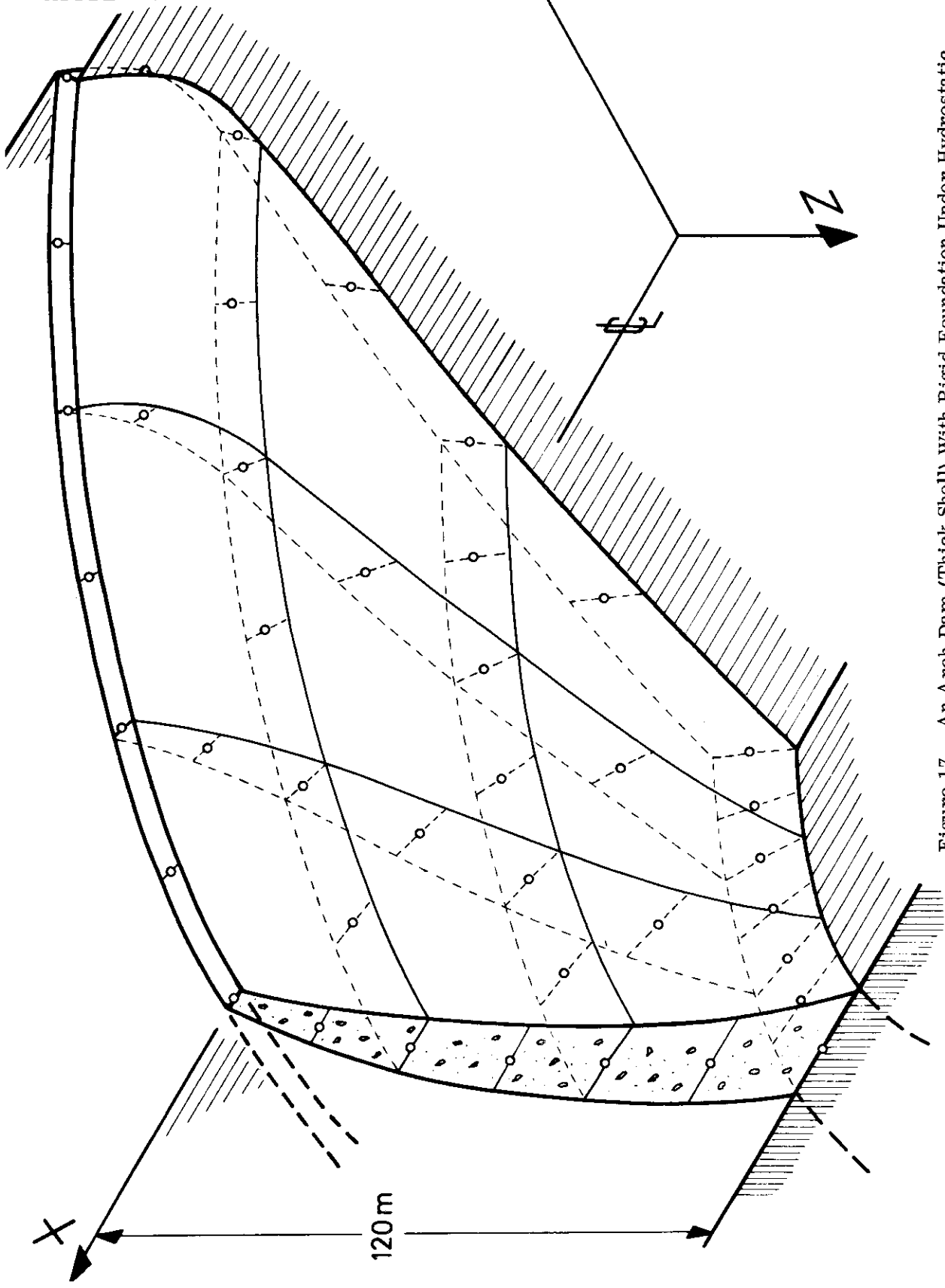


Figure 17. An Arch Dam (Thick Shell) With Rigid Foundation Under Hydrostatic Load. $E = 2 \times 10^5 \text{ kg/cm}^2$, $\nu = 0.15$.

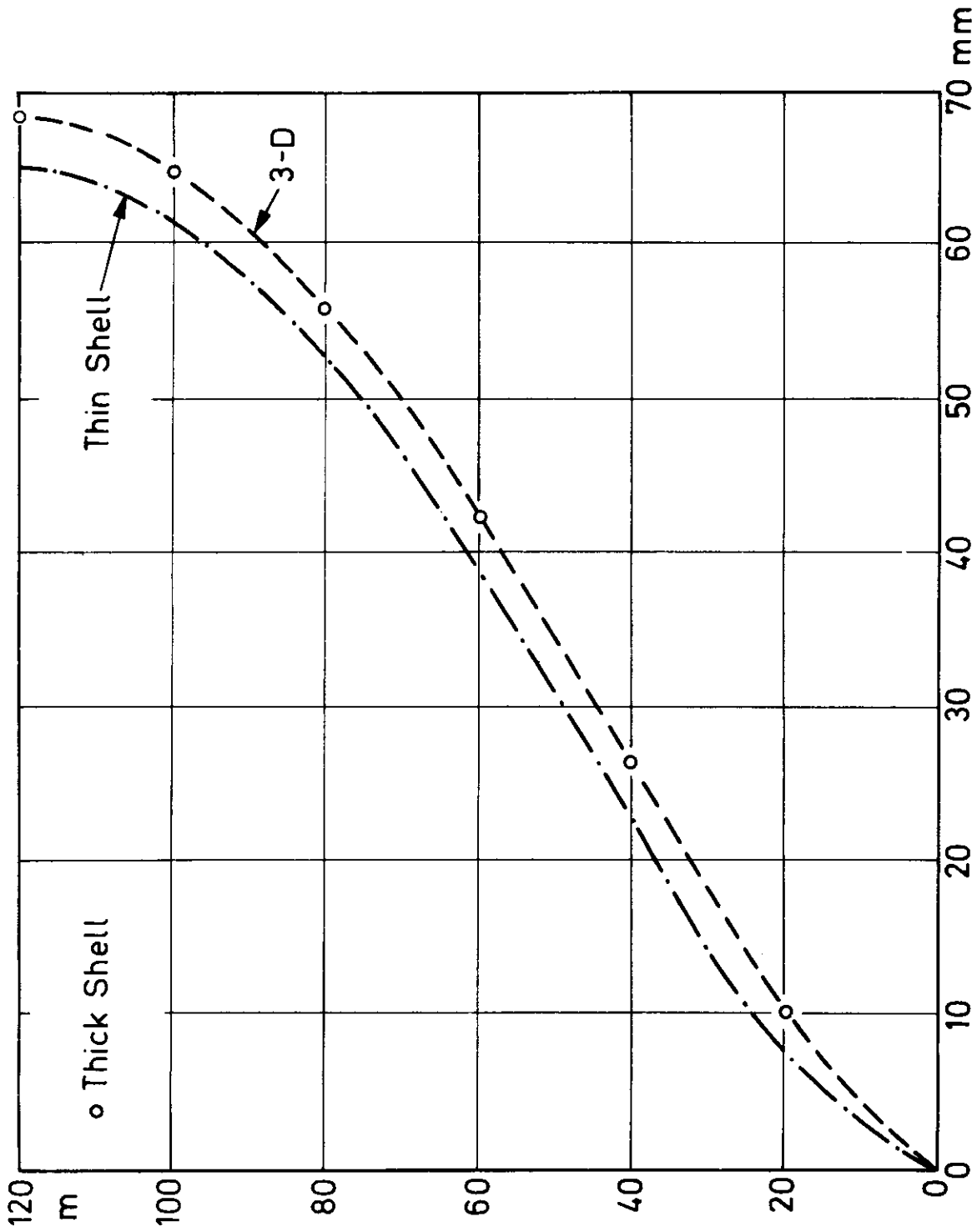


Figure 18. Downstream Displacements of Air Face on Crown Section of Dam. Comparison of Present Solution With Three Dimensional and Thin Shell Solutions of References 4 and 15.

It is of interest also to show a comparable solution based on triangular finite elements and classical thin shell assumptions (Reference 15). The difference of results due to effects of shear deformation now included is significant.

The stress agreement (again for the crown section) is indicated in Figure 19.

SECTION X CONCLUDING REMARKS

The new element has been shown to be capable of dealing adequately with thick as well as thin shells. By virtue of its curved shape it can fit any geometry adequately.

At one end of the scale it duplicates thin shell solutions and is of comparable economy with other elements used in this context. At the other end of the scale, it is capable of dealing with very thick shell situations much more economically than by corresponding two or three dimensional formulations. Its particular use is envisaged in the complex practical situations where thick and thin shell elements are combined with possible membrane regions.

The new element is being incorporated in the NIFE (Numerically Integrated Finite Elements) system developed at University of Wales, Swansea.

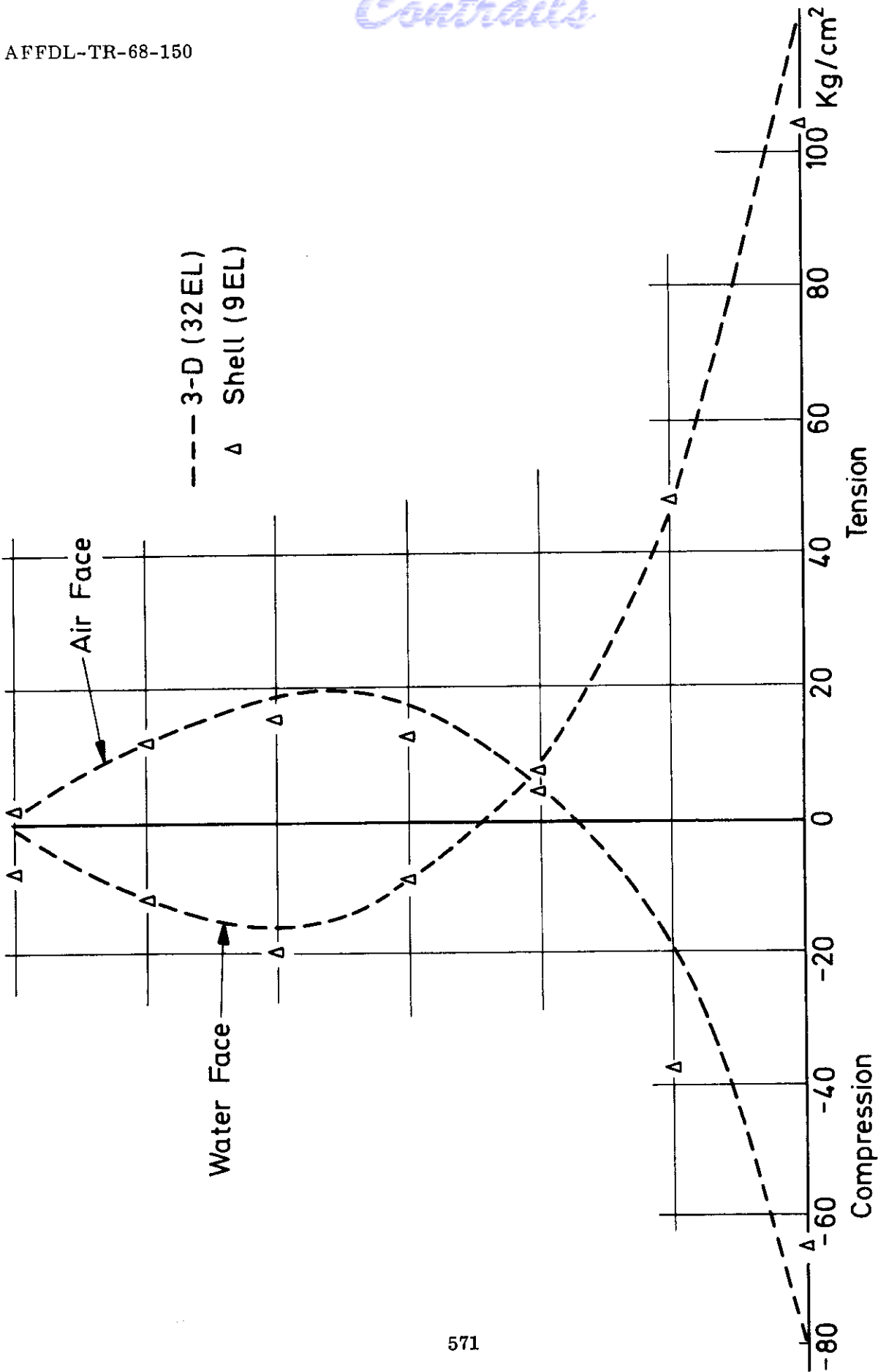


Figure 19. Arch Dam of Figure 17. Comparison of Vertical Stresses (σ_z) on Crown Section

SECTION XI

REFERENCES

1. Irons, B. M., "Engineering Applications of Numerical Integration in Stiffness Method", A.I.A.A.J., Vol. 4, p. 2035-2037, 1966.
2. Irons, B. M., "Numerical Integration Applied to The Finite Element Method", Conference on the use of digital computers in Structural Engineering". University of Newcastle, July 1966.
3. Ergatoudis, J., B. M. Irons, and O. C. Zienkiewicz, "Curved, Isoparametric, Quadrilateral Elements for Finite Element Analysis". Int. J. Solids and Structures, Vol. 4, p. 31-42, 1968.
4. Ergatoudis J., B. M. Irons and O. C. Zienkiewicz, "Three-Dimensional Analysis of Arch Dams and Their Foundations" Symposium on Arch Dams, Inst. of Civil Engineers, London, March 1968.
5. Irons, B. M., and Zienkiewicz, O. C., "The Isoparametric Finite Element System - A New Concept in Finite Element Analysis" Conference on recent advances in stress Analysis, Joint Brit. Comm. Stress Analysis, London, March 1968.
6. Reissner, E., "The Effect of Transverse Shear Deformation on The Bending of Elastic Plates", J. Applied Mechanics, Vol. 12, p. A69-A77, 1945.
7. Zienkiewicz, O. C., and Cheung, Y. K., The Finite Element Method in Structural And Continuum Mechanics, McGraw-Hill, 1967.
8. Grafton, P. E., and Strome, D. R., "Analysis of axi-symmetric shells by the direct stiffness method", A.I.A.A.J., Vol. 1, p. 2342-47, 1963.
9. Percy, J. H., Pian, T. H. H., Klein, S. K., and Navaratna, D. R., "Application of Matrix Displacement Method to Linear Elastic Analysis of Shells of Revolution", A.I.A.A.J., Vol. 3, p. 2138-2145, 1965.
10. Wilson, E. L., "Structural Analysis of Axisymmetric Solids", A.I.A.A.J., Vol. 3, p. 2269-74, 1965.
11. Ahmad, S., Irons, B. M., and Zienkiewicz, O. C., "Analysis of Thick and Thin Shell Structures by General Curved Elements with Special Reference to Arc Dams", (to be published).
12. Timoshenko, S., and Woinowsky-Krieger, "Theory of Plates and Shells", McGraw-Hill, Kōgakusha, 2nd ed., p. 547-554.
13. Ergatoudis, J., Isoparametric Elements in Two And Three Dimensional Analysis, Ph.D. Thesis, University of Wales, 1968.
14. Budiansky, B., and Radkowski, P., "Numerical Analysis of Unsymmetrical Bending of Shells of Revolution", A.I.A.A.J., Vol. 1, p. 1833-1842, 1963.
15. Zienkiewicz, O. C., Parekh, C. J., and King, I. P., "Arc Dams Analysed by a Linear Finite Element Shell Solution Program", Symposium on Arch Dams, Inst. of Civil Engineers, London, March, 1968.